Direct observation of the nonradiative recombination processes in InGaN-based LEDs probed by the third-order nonlinear spectroscopy

Koichi Okamoto*[a], Shin Saijou[a], Yoichi Kawakami[a], Shigeo Fujita[a], Mashahide Terazima[b], Genichi Shinomiya[c], Takashi Mukai[c]

[a]Department of Electronic Science and Engineering, Kyoto University, Kyoto 606-8501, Japan
[b]Department of Chemistry, Graduate School of Science, Kyoto University, Kyoto 606-8502, Japan
[c]Nitride Semiconductor Research Laboratory, Nichia Corporation, 491 Oka, Kaminaka, Anan, Tokushima 774-8601, Japan

ABSTRACT

Nonradiative dynamics of the carriers and/or excitons created by the photoexcitation in InGaN-based light emitting diodes (LEDs) with blue (460nm, 470nm), green (510nm, 540nm), and amber (600nm) emissions were observed by using the transient grating (TG) method which is one of the third-order nonlinear spectroscopy. The dynamics of carries and/or exciton diffusion and dynamics of heat energy released by the nonradiative recombination were observed by the time profile of the TG signals in picosecond and nanosecond time region, respectively. The diffusion coefficients and the temperature change by the heat generation were detected for several LEDs and potted against the peak wavelengths of emission (In composition in active layers). Those results were compared with the results of the time-resolved photoluminescence (PL) spectroscopy. Dependence of In composition on the radiative and nonradiative recombination lifetimes, the luminescence intensities, the internal quantum efficiencies, the heat generation and conduction processes, and the diffusion coefficients of excitons and/or careers were interpreted by the model in terms of the fluctuation and phase separation of In composition.

Keywords: InGaN-based LED, nonlinear spectroscopy, transient grating, nonradiative recombination, carrier dynamics, exciton, diffusion coefficient,

1. INTRODUCTION

InGaN-based semiconductors are very advantageous materials for the light emitting diode (LED) and the laser diode (LD). Recently, InGaN-based LEDs with ultraviolet (UV), [1] blue, green, [2] and amber [3]spectral region and white emission have been fabricated. For LDs, only UV, violet and violet blue emissions have been achieved. Such devices have substantially high emission efficiencies in spite of high threading dislocation density (10^{8}-10^{10} cm^{-2}). This propriety has been interpreted that the created carries and/or excitons should be localized to the potential minima due to the fluctuation of In composition. This property is very advantageous to apply to the bright LEDs. [4] On the other hand, it is not advantageous to LDs because the threshold of LD is increased by such the carriers localization. [5] The external quantum efficiency (η_{ext}) of InGaN-based LED at green spectrum region has been achieved to 10% at room temperature which is comparable to that of ZnCdSe/ZnSe-based LEDs with an etch pit density as low (>10^{4} cm^{2}). However, η_{ext} of LEDs become smaller with more addition of In over 30%.[1] Detailed reason for such saturation of η_{ext} has not so far been elucidated. The optical properties of such photonics devices are controlled by both radiative and nonradiative recombination processes of carriers created by photo-excitation or electron injection. Therefore, to elucidate the correlation between microscopic or nanoscopic structure and recombination mechanism, the carriers dynamics have to be understood clearly. Until now, the most commonly used techniques to characterize optical properties are photoluminescence (PL) and electricluminescence (EL) spectroscopy, which are based on the observation of radiative recombination processes. On the other hand, direct observations of nonradiative dynamics are very difficult and there have been only few reports until now because nonradiative processes do not involve the photon transition. Such nonradiative processes are very impotent to elucidate the optical properties and to develop the quality of photonics devices. For example, diffusion and nonradiative recombination processes of carriers and/or exciton are very important processes which affect the optical properties.

Recently, we proposed that the transient grating (TG) method which is one of the third-order nonlinear spectroscopic technique is powerful tool to detect the thermal dynamics of nonradiative recombination processes by using ZnSe-based semiconductors and bulk GaN.[6-7] In this paper, these methods were developed to observe both the spatial diffusion

* Correspondence: Email: kokamoto@vbl.kyoto-u.ac.jp; Telephone: +81-75-753-7577; Fax: +81-75-753-7579

processecs and the nonradiative recombination processes of carrires and/or excitons in InGaN/GaN/AlGaN-based LEDs emitting at the blue to amber spectral region. By using this result, the saturation phenomena of η_{ext} value over the green spectral region is discussed.

2. METHOD

The sample of InGaN/GaN/AlGaN-based LEDs were fabricated by Nichia Corporation. These LEDs were grown by the two-flow metalorganic chemical vapor deposition (MOCVD) method on a (0001) C-face sapphire substrate. The device structures consisted of a 30nm GaN buffer layer, a 5μm-thick layer of n-type GaN:Si, a 3nm-thick active layer of undoped InGaN, a 60nm-thich layer of p-type AlGaN:Mg, and a 150nm-thick layer of p-type GaN:Mg. The active region was a single quantum well (SQW) structure. The peak wavelength of these LEDs are blue (460nm, 470nm), green (510nm, 540nm), and amber (600nm). In compositions are roughly estimated to 30% - 80% according to the growth condition that may be overestimated if the recent reported value of bowing parameter for the InGaN alloys is adopted to account for the emission energies.

The principle and the setup of the TG method have already been descried.[6-7] Configuration of the excitation and probe beams of the TG method are shown in Fig. 1. The interference pattern is created by crossing two excitation beams in the sample materials. Then, the light intensity in the crossing region is modurated (Optical grating). The sample is excited by this optical grating and the carriers and/or excitons are created. Then, the carrier densities are also modurated along the optical grating (population grating). The excited area releases the heat by the nonradiative recombination of carriers and/or excitons and the temperature of the sample is modulated (thermal grating). The refractive index (n) and the absorbance (k) of the materials are also modulated by these grating. Such modulation of optical properties (Δn, Δk) are similar to the refractive grating. A probe beam was partly diffracted (TG signal) by these gratings. The intensity of the TG signal can be written by

$$I_{TG} = \alpha \Delta n^2 + \beta \Delta k^2 \qquad (1)$$

where α and β are constants. If samples are transparent at the probe wavelength, I_{TG} can be written only by the term of Δn. After the excitation, the population grating and the thermal grating are relaxed by the diffusion of excitons and/or carriers and heat conduction, respectively. The photo induced change of refractive index δn (x, t) due to the population grating and the thermal grating were given as a function of time(t) and space(x), where

$$\delta n(q,t) = \frac{dn}{dN}\delta N(q,t) + \frac{dn}{dT}\delta T(q,t) \qquad (2)$$

dN and dT show the carrier density change and the temperature change between the bright region and the dark region in the grating, respectively. Therefore, the diffusion processes and heat conduction can be observed by the time profile of the TG signals. The first and second terms in eq. (2) are contributed from the population grating and from thermal grating, respectively. When the two components contribute simultaneously to the TG signal, the analysis of the TG signals should be very difficult. However, the carrier diffusion and heat conduction take place at quite different time scale. So, the thermal grating component and population grating component in the TG signal can be separated in the time scale by changing the population of excitation laser and the fringe space of the grating, the latter parameter of which can be controlled by the adjustment of the cross angle of two excitation beams. When the diffusion length is narrow, the population grating can decay faster than the nonradiative recombination process and thermal grating can not generate effectively.

To detect the heat generation as a result of nonradiative recombination processes, frequency tripled beam of a Q-switch Nd:YAG laser (Spectra-Physics GCR-170-10; λ=355nm) and continuous wave beam of HeNe laser (633nm) were used for excitation and probe beam, respectively. Pulse width and repetition rate of excitation are 10ns and 5Hz, respectively. The experimental setup for the TG measurement with nanosecond pulsed laser is shown in Fig. 1. The fringe space and the crossing angle between two excitation beams are in the range 14μm and 1°, respectively. The TG signal was detected by a photomultiplier tube (Hamamatsu R-928).

To detect the diffusion processes of excitons and/or carries, frequency doubled beam (388nm) and fundamental beam (755nm) of a fiver laser (Clark CPA-2001) were used for excitation and probe beams, respectively. Pulse width and repetition rate of excitation are 500fs and 1kHz, respectively. Photograph of the measurement system of the TG method with sub-picosecond laser system is shown in Fig. 2, where optical pass are schematically drawn and optical components are described. The fringe space and the crossing angle between two excitation beams are 0.7μm and 30°. The TG signal was detected by a photomultiplier tube and averaged with a boxcar-integrator (EG&G Model 4400).

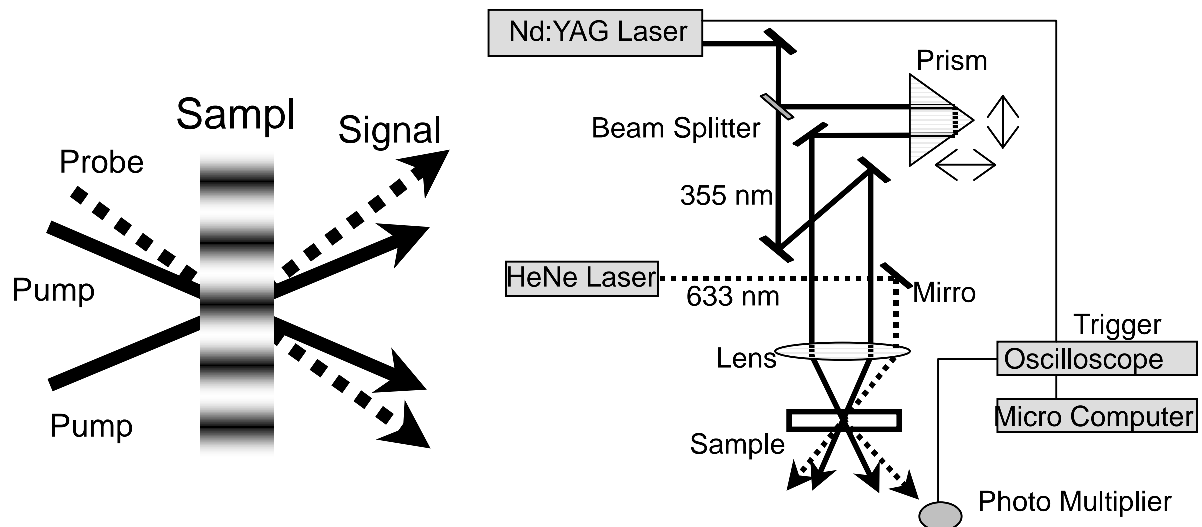

Fig. 1 Configuration of the excitation beam and probe beam of the transient grating method (left) and the experimental setup with nanosecond pulsed laser (right).

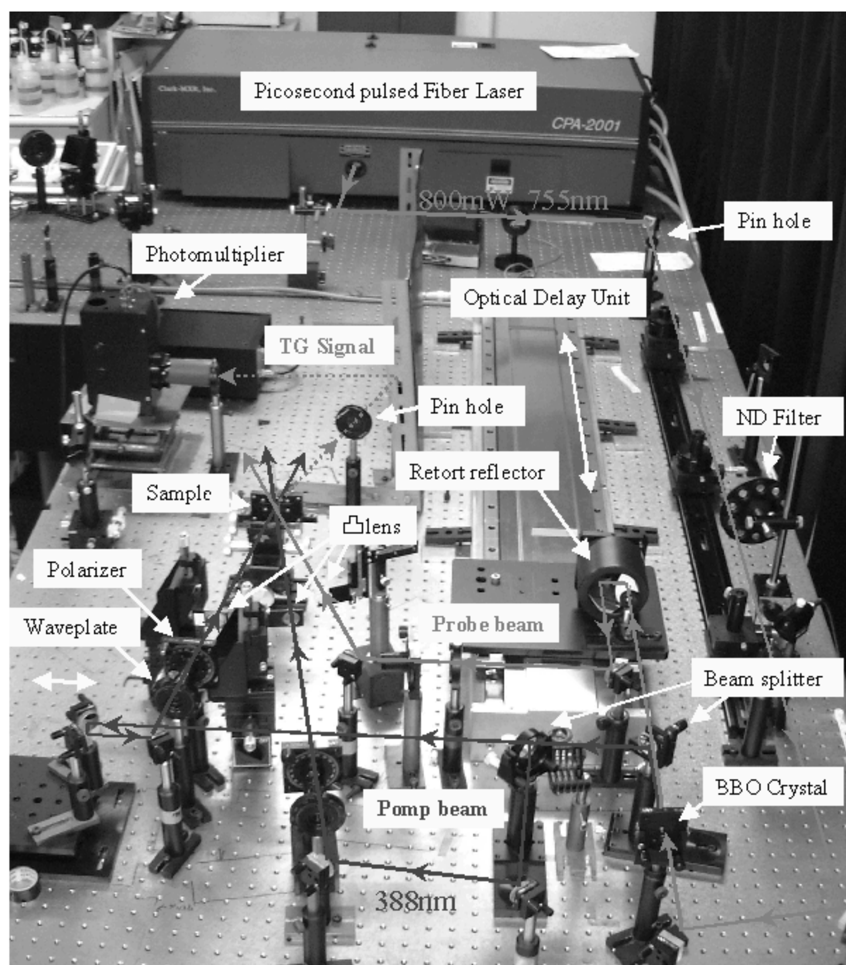

Fig. 2 Photograph of the measurement system of the transient grating method with sub-picosecond pulsed laser.

For time-resolved photoluminescence (TRPL) measurement, the frequency doubled beam of a mode-rocked Ti: sappier laser (Spectra-Physics; λ=370nm) which was pumped by Ar^+ laser was used for excitation. Pulse width and repetition rate of excitation are 1.5ps and 80MHz, respectively. The signals were detected by the monochromator and streak camera (Hamamatsu).
The whole measurements have been done at room temperature (23°C).

3. RESULT AND DISCUSSION

3.1 Time-resolved photoluminescence measurement with picosecond pulsed laser

Firstly, we measured the radiative processes by using the TRPL with picosecond pulsed laser. Fig. 3 (a) shows the In composition dependence of the PL intensities and of internal quantum efficiencies at room temperature. This tendency is similar to the published data on the emission wavelength dependence of the external quantum efficiencies driven under 20 mA. In the UV region, emission intensities become higher with increasing the In contents. On the other hand, in the case of LEDs used this paper, in the visible region (longer than 460nm), emission intensities decreased with increasing the In composition. The emission intensities are controlled by both the radiative and nonradiative recombination processes. The photoluminescence lifetime (τ_{PL}) obtained by the TRPL was also plotted in Fig. 3 (b). It was found that the τ_{PL} becomes longer with increasing of In contents. τ_{PL} consists of the radiative recombination lifetime (τ_{rad}) and the nonradiative recombination lifetime ($\tau_{non\text{-}rad}$) as follows,

$$\frac{1}{\tau_{PL}} = \frac{1}{\tau_{rad}} + \frac{1}{\tau_{non-rad}} \tag{3}$$

The internal quantum efficiency (η_{int}) of the emission can be also written in terms of τ_{rad} and $\tau_{non\text{-}rad}$

$$\eta_{\text{int}} = \frac{\tau_{non-rad}}{\tau_{rad} + \tau_{non-rad}} \tag{4}$$

When the luminescence intensity η_{int} is constant in a low temperature region and then decreases gradually with increasing temperature, it can be assumed that η_{int} is nearly equal to unity at low temperature region. Therefore, η_{int} at room temperature can be obtained and it was also plotted in Fig. 3 (a).[8] η_{int} also decreases with longer wavelength. From obtained vale and eq. (4), τ_{PL} can be separated to τ_{rad} and $\tau_{non\text{-}rad}$ and plotted in Fig. 3 (b). It was found that τ_{PL} is nearly equals to $\tau_{non\text{-}rad}$ and τ_{rad} of amber LED emitting at 600nm is much longer than another one.

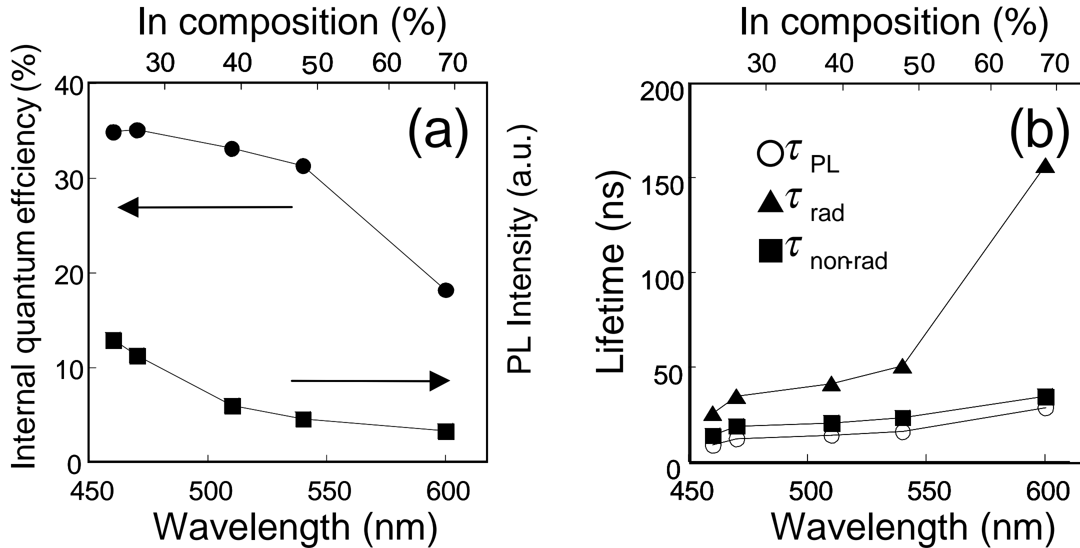

Fig. 3 In composition dependence of the photoluminescence intensities and internal quantum efficiency (left) and the PL lifetime (○), radiative (▲) and nonradiative (■) recombination lifetime (right).

3.2 Transient grating measurement with sub-picosecond pulsed laser

Typical time profile of the TG signal with sun-picosecond pulsed laser was shown in Fig. 4. The TG signals decayed with few tens picosecond. The similar signals could be observed by another LEDs. The rise and decay of this signal should be attribute to the generation and diffusion processes of the excitons and/or carriers. The rise component of this signal was similar to the excitation pulse shape. The generation processes should be much faster than the excitation pulse width. The carrier dynamics can be written by the following rate equations,[7]

$$\frac{dN(x,t)}{dt} = D\frac{\partial^2 N(x,t)}{\partial t} - \left(\frac{1}{\tau_{rad}} + \frac{1}{\tau_{on-rad}}\right)N(x,t). \qquad (5)$$

By solving the rate equations, the time profile of the TG signal within picosecond time region was obtained as follows.

$$\delta N(q,t) = N(q,0)\exp\left[-Dq^2 t - \left(\frac{1}{\tau_{rad}} + \frac{1}{\tau_{on-rad}}\right)t\right], \qquad (6)$$

where $\delta N(q, t)$ is the Fourier component of $\delta N(x, t)$. Observed decay of the TG signals [few hundred picosecond (Fig. 4)] were much faster than that of the PL signals [few tens nanosecond (Fig. 3)]. Therefore, in this case, Λ=0.7μm ($q=2\pi/\Lambda$), the diffusion processes of carriers are much faster than the recombination processes ($1/\tau_{rad}+1/\tau_{non\text{-}rad} << Dq^2$). Under this condition, decay rate constant should be due to only Dq^2 term. The obtained time profile can be fitted by the single exponential function. We can obtain the diffusion coefficient by eq. (6). Obtained D values were plotted in Fig. 5. It was found that the D become faster with increasing In contents.

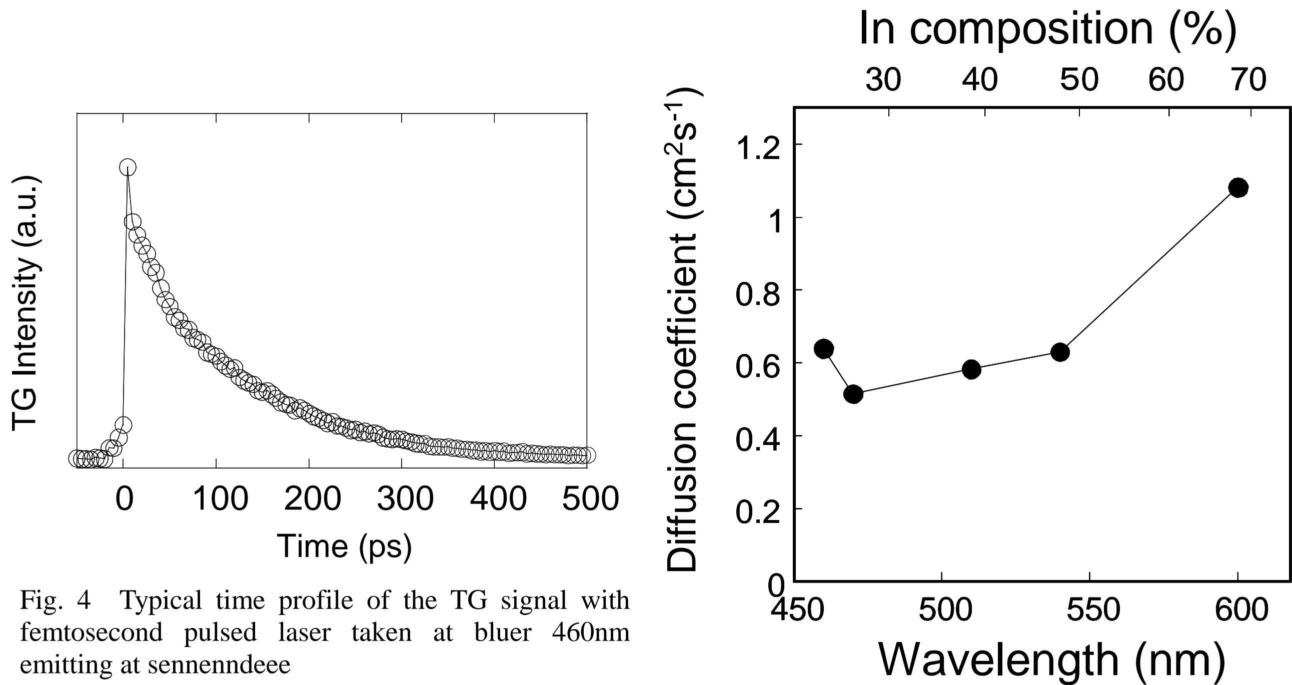

Fig. 4 Typical time profile of the TG signal with femtosecond pulsed laser taken at bluer 460nm emitting at sennenndeee

Fig. 5 In composition dependence of the diffusion coefficients (D) of carriers and/or excitons.

3.3 Transient grating measurement with nanosecond pulsed laser

Typical time profile of the TG signal with nanosecond pulsed laser is shown in Fig. 6. This signal rise immediately within the excitation pulse (10 ns) and decay within few tens nanosecond. This signal also should be due to both the population grating and/or thermal grating. However, with few tens nanosecond region after excitation, the excitons or carriers should be already terminated. Therefore, the obtained TG signal should be due only to the thermal grating.

To analyze the time profile of the TG signals, the time profile of the carrier dynamics should be considered. Then, the temperature change $\delta T(x, t)$ by the nonradiative recombination of the carriers are given by

$$\frac{d\delta T(x,t)}{dt} = a\frac{1}{\tau_{on-rad}}\delta N(x,t) + D_{th}\frac{\partial^2 \delta T(x,t)}{\partial t} \tag{7}$$

where, D_{th} is thermal diffusivity in the materials and a is the proportional constant. By solving this equation with condition $D>>D_{th}$, following relationship is obtained.

$$\delta T(q,t) = \frac{a\dfrac{1}{\tau_{on-rad}}N(q,0)}{\dfrac{1}{\tau_{rad}} + \dfrac{1}{\tau_{on-rad}} + Dq^2}\left\{-\exp(-Dq^2 t) + \exp(-D_{th}q^2 t)\right\} \tag{8}$$

where $\delta T(q, t)$ is the Fourier component of $\delta T(x, t)$. In this case, Λ=14μm ($q=2\pi/\Lambda$), the diffusion processes of carriers are slower than the recombination processes ($1/\tau_{rad}+1/\tau_{non-rad}>> Dq^2$) and faster than the thermal conduction ($D >> D_{th}$), Eq. (8) can be reduced as simple exponential function. Accordingly, we could observe the carrier diffusion and thermal processes selectively by changing the crossing angle of excitation beams and the time scale.

Eq. (8) indicates that from the pre-exponential factor and the decay rate constant, we can obtain the amount of heat released by the nonradiative recombination and D_{th}. The time profile of the TG signals in Fig. 6 could be fitted by using the single exponential function. D_{th} is obtained and plotted in Fig. 7 (a). With increasing In composition, D_{th} becomes smaller slightly. D_{th} can be calculated theoretically by $D_{th}=\lambda_c/\rho C_p$. By using the literature values (λ_c=1.3 $Wcm^{-1}K^{-1}$, ρ=6.095 gcm^{-3}, and C_p=9.745 $calmol^{-1}K^{-1}$ as GaN), D_{th} was calculated as D_{th}= 0.44 cm^2s^{-1} for bulk GaN. This value is near to the experimental one. Estimated D_{th} values for LEDs are smaller than that of GaN. This is partly because the heat generation is partly contributed from InGaN active layers as well as AlGaN cladding layers. However, it should be notes that the D_{th} value differs also with carrier densities and with dislocation densities. Therefore, more detailed analysis are needed for further discussion. Fig. 7 (b) shows the intensities of the TG signals which is proposed to amount of heat released by the nonradiative recombination.

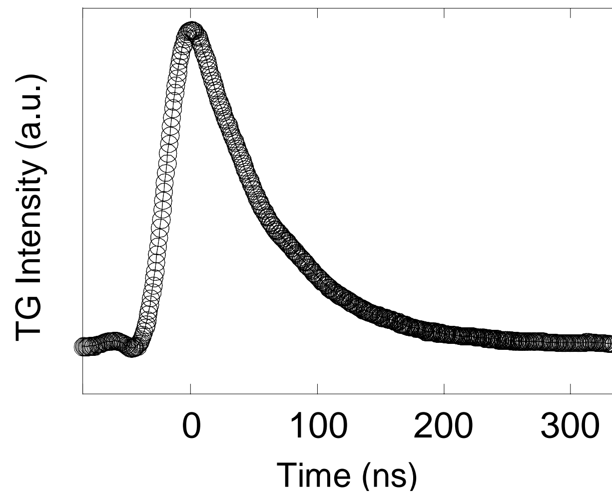

Fig. 6 Typical time profile of the TG signal with nanoosecond pulsed laser taken at blue emitting at 460nm

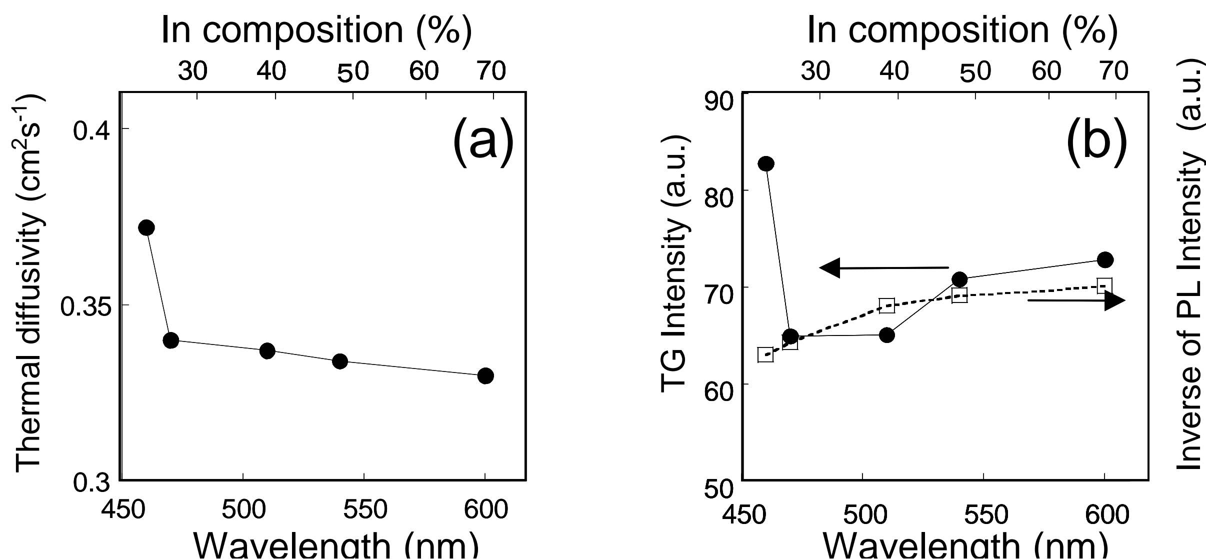

Fig. 7 In composition dependence of the thermal diffusivity (Dth) (left) and TG intensities which in proportional to the amount of heat released by the nonradiative recombination (●) and invers of PL intensities (Shownin) (doted line).

3.4 A model of carrier dynamics

It was found that the PL intensities and the internal quantum efficiencies become smaller with increasing In mole fractions (x) in $In_xGa_{1-x}N$ active layers larger than 30 % . It has been reported that an addition of In to GaN up to about 30 % results in the enhancement of emission efficiencies. This could be interpreted as two mechanisms. The first mechanism is that an addition of small amount (a few %) of In is very effective for the reduction of nonradiative recombination centers, origins of which arises from point defects. Another one plays a major role in the layers with x>10 %, where fluctuation of In composition leads to the localization centers of excitons. Such a localization effect acts as positive factor for the improvement of the emission efficiencies because the pathway to the nonradiative recombination centers are prohibited once excitons are trapped in small volume. However, it was known that when In composition become too large, the PL intensities and the internal quantum efficiencies become smaller. The turning point is about 30 % for In composition and 460 nm (blue) for wavelength. In this study, we focused to the region over the turning point. As depicted in Fig. 3 (b), nonradiative recombination lifetimes gradually increase from 10 ns to 30 ns with increasing emission wavelength. This result suggests that the probability of nonradiative recombination pathway lowered with wavelength, contributing as a positive factor for the emission efficiencies. The probability of nonradiative processes are contributed by three terms, namely, the thermal velocity of carriers and/or excitons, density of nonradiative recombination centers, and capture cross section to the nonradiative centers. Therefore, the increase of nonradiative lifetimes with wavelength itself can not solely be ascribed to the reduction of nonradiative centers due to improvement of crystal qualities. However, the diffusion coefficients of carriers and/ or excitons decreases slightly from 0.61 at 460 nm to 0.52 at 470 nm, and then increases with wavelength above 470 nm as shown in Fig. 5. This may suggest the reduction of nonradiative centers. Radiative lifetimes also increase with wavelength. A dramatic increase of radiative lifetime was observed from 50 ns at 540 nm to 150 ns at 600 nm. Accordingly, it was clarified that the declination of emission efficiencies over x=30 % is limited by the reduction of oscillator strength of excitons. The oscillator strength is determined from the number of excitons that satisfy the momentum conservation law with photon, as well as from the overlap integral of wavefunctions between electrons and holes. The former term is related to the dimensionality of excitons because the thermalization of excitons with higher momentum changes with the density of states of excitons. The latter term is strongly related to the internal electric field caused by the effects of piezo and spontaneous polarization. Since the internal electric field is enhanced with increasing In mole fraction, electrons and holes are separated each other perpendicular to the well layer. This effect contributes at least in part to the reduction of oscillator strength. Nevertheless, the measurements of lifetimes on the temperature dependence would give more clear information on radiative recombination processes of each sample. So far, detailed measurements have been performed only for blue LED emitting at 460 nm. The results show that the radiative lifetimes were almost constant at about 5 ns from 20 K to 300 K indicating the zero-dimensionality of excitons, where excitons are confined within the volume with diameter less than 3 nm.

As mentioned before, the diffusion coefficient reaches to the minimum at about 470 nm, and increases again with wavelength. This fact suggests that the localization of carriers and/or exciton become weaker with increasing the In mole fraction more than 30 %. It appears that this tendency is not consistent with the model of exciton localization because the degree of phase separation would be enhanced with increasing the mean value of In mole fraction incorporated to the layer. In fact, preliminary results on fluorescent microscopic measurement indicates that the inhomogeneity of the emission colors become pronounced with mole fraction more than 30 %. However, these results are with the scale of about micron resolution. Since the recombination of carriers or excitons take place within the scale less than about 0.1 μm, it may be important to improve the spatial resolution, for instance by using near field optical technique for further discussion. We speculated that the homogeneity of In composition may be improved with mole fraction in the scale within the recombination pathways, but is degraded in the more macroscopic scale. As shown in Fig. 7 (b), TG intensity and inverse of PL intensity is well correlated each other besides the data point at 460 nm. The reason for the discrepancy at 460 nm is not clear at a moment. However, this may be related to the experimental condition in which the photo-excitation was made not only to the well layer, but also mainly to the GaN cladding layer. In such case, photo-generated carriers and/or excitons may be captured by nonradiative recombination centers before reaching at the InGaN active layer. The measurement of TG-signal due to thermal process is now under progress with a selective photo-excitation condition. Another important approach would be the quantitative measurements of TG spectroscopy depending on temperature. Such assessment would give clear guideline whether or not internal quantum efficiencies can be assumed to unity at low temperature.

4. CONCLUSION

The transient grating method was used to detect the nonradiative dynamics which have been very difficult to detect. The diffusion processes of carriers and/or exciton and thermal dynamics released by the nonradiative recombination process were observed selectively by changing the excitation pulse width and the crossing angle of two excitation beams. It was found that the diffusion coefficients of carriers and/or excitons become faster and thermal diffusivity become slower with increasing of In composition. We proposed that the phase description to In rich region and In poor region should be created at the too many addition of In.

ACKNOWLEDGMENTS

This work was partly supported by the Kyoto University-Venture Business Laboratory Project, Research Foundation for Opto-Science and Technology, Konica Imaging Science Foundation and a Grant-in- Aid for Scientific Research from the Japan Society for the Promotion of Science and Ministry of Education, Science and Culture.

REFERENCES

1. T. Mukai, S. Nakamura, "Ultraviolet InGaN and GaN singl-quantum-well-structure light-emitting diodes grpwn on epitaxial laterally overgrown GaN substrates", Jpn. J. Appl. Phys. **38**, 5735-5739, 1999.
2. T. Mukai, M. Yamada, S. Nakamura, "Current and temperature dependences of electroluminescence of InGaN-based UV/blue/green light-emitting diodes", Jpn. J. Appl. Phys. **37**, L1358-L1361, 1998.
3. S. Nakamura, M. Senoh, N. Iwasa, S. Nagahama, T. Yamada and T. Mukai, "Amber InGaN-based light-emitting diodes Operable at high ambient temperatures", Jpn. J. Appl. Phys. **37**, L479-L481, 1998.
4. Y. Kawakami, Y. Narukawa, K. Sawada, S. Saijyo, Sz. Fujita, Sg. Fujita, S. Nakamura, "Recombination dunamics of localized excitons in self-formed InGaN quantum dits", Materials Science $ Engineering **B50**, 256-263 (1997)
5. Y. Narukawa, Y. Kawakami, M. Funato, Sz. Fujita, Sg. Fujita, S. Nakamura, "Role of self-formed InGaN quantum dots for exciton localization in the purple laser diode emitting at 420nm", Appl. Phys. Lett **70**, 981-983 (1997)
6. K. Okamoto, Y. Kawakami, Sg. Fujita, M. Terazima, "Photothermal processes of wide-bandgap semiconductors probed by the transient grating method" Analytical Science, *in press.*
7. K. Okamoto, Y. Kawakami, Sg. Fujita, M. Terazima, S. Nakamura, "Nonradiative Recombination Processes in GaN-based Semiconductors Probed by the Transient Grating Method", Jpn. J. Appl. Phys., *in press.*
8. R. C. Miller, D. A. Kleinman, W. A. Nordland Jr., A. C. Gossard, "Luminescence studies of optical pumped quantum wells in GaAs-$Al_xGa_{1-x}As$ multiple quantum wells", Phys. Rev. **B22**, 863-871 (1980)